 doi:10.20944/preprints201710.0019.v1

Article

Nanoindentation-induced Pile-up in the Residual Impression of Crystalline Cu with Different Grain Size

Jiangjiang Hu [1], Yusheng Zhang [2,*], Weiming Sun [3] and Taihua Zhang [1]

[1] College of Mechanical Engineering, Zhejiang University of Technology, Hangzhou 310014, China; jiangjiangwho@gmail.com (J. Hu); zhangth@zjut.edu.cn (T. Zhang)

[2] Advanced Materials Research Center, Northwest Institute for Non-Ferrous Metal Research, Xi'an, 710049, China

[3] Key Laboratory of Automobile Materials, College of Materials Science and Engineering Jilin University, Nanling Campus, Changchun 130025, China; sunwm15@mails.jlu.edu.cn (W. Sun)

* Correspondence: y.sh.zhang@163.com

Abstract: At room temperature, the indentation morphologies of crystalline copper with different grain size including nanocrystalline (NC), ultrafine-grained (UFG) and coarse-grained (CG) copper were studied by nanoindentation at the strain rate of 0.04/s without holding time at indentation depth of 2000 nm. As the grain size increasing, the height of the pile-up around the residual indentation increases and then has a slightly decrease in the CG Cu, While the area of the pile-up increases constantly. Our analysis has revealed that the dislocation motion and GB activities in the NC Cu, some cross- and multiple-slips dislocation insides the larger grain in the UFG Cu, and forest dislocations from the intragranular Frank-Read sources in the CG Cu, would directly induce these distinct pile-up effect.

Keywords: Nanoindentation; Pile-up effect; Grain size; Dislocation motion; Grain boundaries activities

---

1. Introduction

Nanoindentation technique has been widely used to characterize the mechanical properties of bulk- and thin-film materials on nano- and microscopic scales such as elastic modulus (E) and hardness (H). From the experimental load-displacement curves, three vital quantities can be obtained: the maximum load P_{max}, the maximum displacement h_{max}, and the contact stiffness S [1]. Then the projected contact area A is calculated from the contact depth using the calibrated area function and then the final E and H can be obtained. It should be noted that the involved mechanical parameters in this contact area calibration are acquired from the indentation of a standard fused silica sample. But in some cases, deviations are evidently generated in the indentation process itself when the mechanical behaviors between the studied materials and the standard sample are quite different. For example, there is an apparent upward extrusion at the edge of the contact with the indenter in some metals, known as pile-up, which means the actual contact area is larger than the value calculated by the Oliver-Pharr method [1]. Some studies has reported that the true contact area is 60% larger than the measured value as serious pile-up occurs, leading to the overestimation of the E and H [2-7]. Therefore, it is invaluable in quantitatively accounting for the pile-up influence on E and H in the various materials and loading conditions under nanoindentation testing.

Preprints (www.preprints.org) | NOT PEER-REVIEWED | Posted: 3 October 2017 doi:10.20944/preprints201710.0019.v1

Many studies have shown that the formation of pile-up is closely related with the ratio of the yield stress (σ_y) to *E*, the ratio of the final indentation depth h_f to h_{max}, and the strain hardening exponent (*n*). Metallic materials with smaller values of the σ_y / E and *n* usually exhibit larger pile-up height, but accurately determined these two parameters in the indentation process becomes impossible. Therefore, the easily measured h_f / h_{max} from the load-displacement curve can be used to determine the prevalence of the pile-up. It has been suggested that for the materials with low work hardening ability, the amount of the pile-up would become obvious as the ratio of h_f / h_{max} is larger than 0.7 [2, 3]. Interestingly, most of the theoretical development reports were based on numerical modelling [5, 8-12], with very limited experimental data being used to explain this phenomena. Although some reports have studied the effect of work-hardening, grain orientation on the pile-up formation in the metals [3, 13], other factors such as grain size and deformation mechanisms transformation have not been mentioned.

The aim of the present work is to establish the relationship between the pile-up effect and grain size in the crystalline materials. Nanocrystalline (NC), ultrafine-grained (UFG) Cu and coarse-grained (CG) copper samples were detected by the nanoindentation at room temperature at indentation depth of 2000 nm, and their pile-up effect around the residual impressions were systemically studied. Deformation mechanism transformation is used to explain why the pile-up effect exhibits different morphologies in the crystalline materials with different grain sizes.

2. Experiments details

Bulk NC/UFG Cu specimens with different grain sizes used in this article were synthesized by electric brush-plating on the substrate of copper sheets with bath only containing $CuSO_4{\cdot}5H_2O$ (180-220g/l), and the detailed processes are presented in the refs. [14-16]. A commercial coarse-grained (CG) copper sheet with thickness of 2 mm and purity of 99.99 wt.% were annealed at a temperature of 800 ^oC for 24 h, prepared for a contrastive experiment. Foil samples for transmission electron microscope (TEM, JEM-2100F) observation under accelerating voltage of 200 kV were prepared by cutting, polishing and dimpling by argon-ion milling (EMRES101) at 5 kV. Square-shaped nanoindentation specimens of NC/UFG/CG Cu with gauge size of 30×30×2 mm^3 were cut, and then mechanically grinded with SiC papers, and finally polished with a microcloth using a slurry of 0.5 μm alumina. To acquire reliable nanoindentation data, the surface of the test specimens were mechanically polished to mirror finishing, and then their mechanical properties were characterized at room temperature by a nanoindenter (Agilent-G200) with a Berkovich diamond indenter. All the samples were loaded at strain rates of 0.4/s, 0.04/ and 0.004/s to the indentation depth of 2000 nm without holding time under the procedure of the continuous stiffness measurement (CSM). The thermal drift rate prior to testing was limited below 0.025 nm/s and the indentation under same condition was repeated at least ten times. The surface morphology of the residual impression obtained at strain rate of 0.04/s was observed by the laser confocal microscopy (LSM, OLS4500).

3. Results

3.1 TEM observation

Fig. 1 gives the TEM bright images of the typical microstructures of the as-brush-plated NC/UFG Cu. It reveals that these materials consist of uniformly equiaxed grains with random crystalline orientations and predominant high-angle grain boundaries (GBs). Grain size was measured from the statistical analysis of 500 grains taken from the several TEM images, and the average values of these materials are 30 nm, 150 nm and 300 nm, respectively.

Preprints (www.preprints.org) | NOT PEER-REVIEWED | Posted: 3 October 2017 doi:10.20944/preprints201710.0019.v1

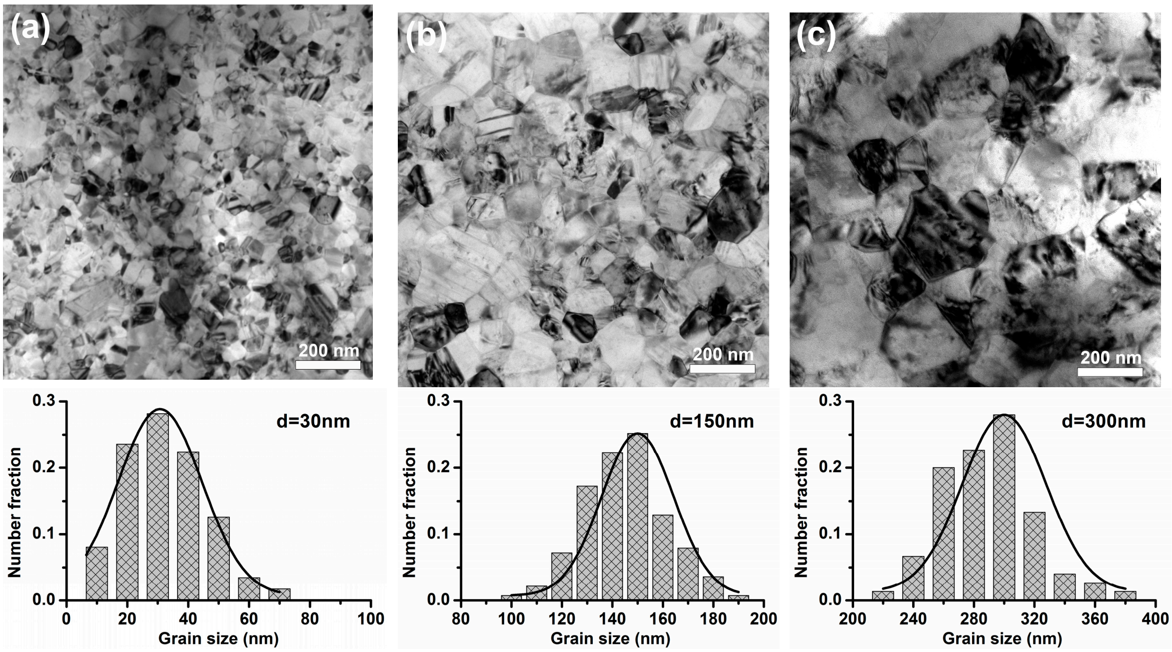

Fig. 1 TEM bright-field images of the as-brush-plated NC/UFG Cu: (a) 30 nm Cu; (b) 150 nm Cu; (c) 300 nm Cu.

3.2 Mechanical properties of the nanoindentaiton

Fig. 2a shows the load-displacement (*P-h*) curves obtained at strain rate of 0.04/s to the indentation depth of 2000 nm without holding time on these four materials. It can be seen that as the grain size decreases, the acquired load at given displacement in the loading stage increases rapidly and the slope value of the *P-h* curves during the unloading regime decreases obviously. To assess the effect of the pile-up in the indenters, Table 1 summarizes the ratio of h_f/h_{max} in these four materials, where h_f and h_{max} are the final and maximum displacement at zero and highest load in the *P-h* curves. Clearly, this ratio decreases constantly as the grain size decreases.

Fig. 2b gives the corresponding *E* and hardness *H* versus displacement curves. It can be found that the measured *E* of these four materials is independent of displacement after the indentation depth is over 500 nm and their values are in the range of 120~135 GPa. The *H* value increases rapidly at given displacement as the grain size decreases. To give a quantitative measurement of the strain rate dependence of hardness in the different materials, the strain rate sensitivity (*m*) obtained by the equation of $m = \partial \log H / \partial \log \varepsilon_L$ is used. Fig. 3 gives the *m* of the NC/UFG/CG Cu obtained at three typically different loading strain rates of 0.4/s, 0.04/s and 0.004/s. The *m* value increases with decreasing the grain size and the values in these four materials are 0.08557, 0.05978, 0.04899 and 0.01104, respectively.

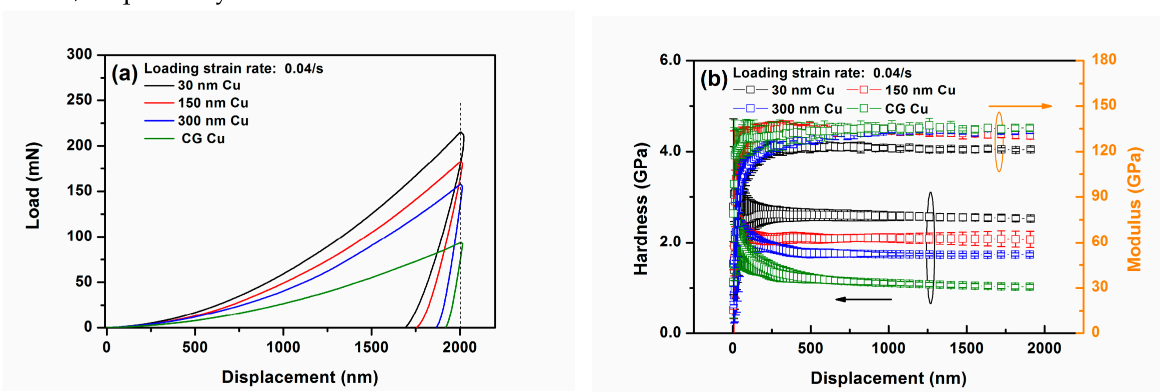

Preprints (www.preprints.org) | NOT PEER-REVIEWED | Posted: 3 October 2017 doi:10.20944/preprints201710.0019.v1

Fig. 2 (a) Several load-displacement (*P*-*h*) curves obtained at indentation depth of 2000 nm at ε_L of 0.4/s in the four NC/UFG/CG Cu. (b) Elastic modulus (*E*) and hardness (*H*) versus displacement curves of 30 nm, 150 nm, 300 nm and CG Cu measured by the CSM method at ε_L of 0.04/s.

Table 1 h_f/h_{max} of NC/UFG/CG Cu obtained at strain rate of 0.04/s and indentation depth of 2000 nm.

Materials	h_{max} at P_{max}	h_f at 0 mN	h_f/h_{max}
30 nm Cu	2000 nm	1694 nm	0.847
150 nm Cu	2000 nm	1756 nm	0.878
300 nm Cu	2000 nm	1867 nm	0.934
CG Cu	2000 nm	1919 nm	0.960

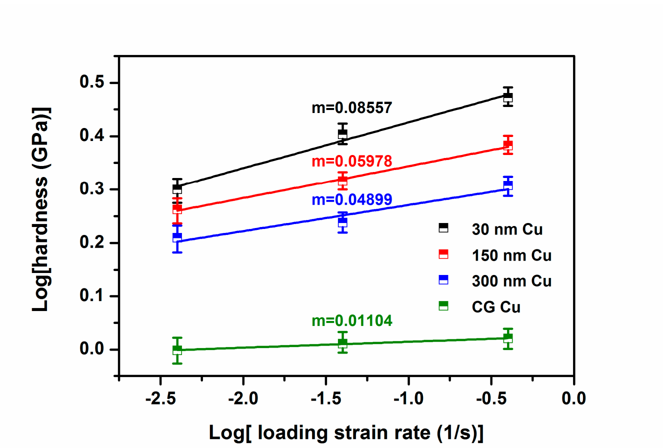

Fig. 3 The hardness versus loading strain rate ($\log H - \log \varepsilon_L$) curves for measuring the strain rate sensitivity (*m*) of NC/UFG/CG Cu measured at three different ε_L of 0.4/s, 0.04/s and 0.004/s.

3.3 Residual morphology of the impression

LCM images can be used to determine the extent and nature of the pile-up in the deformed surface topography of the impression. Fig. 4 gives of the residual morphology of the Berkovich indenter after loading at strain rate of 0.04/s at same indentation depth of 2000 nm in these four NC/UFG/CG Cu samples. Clearly, expect the indents of 30 nm Cu exhibiting very little protrusion, the other three materials appear obvious pile-up effect in the vicinities of the impression. In order to quantify the pile-up height along the z-axis in the impression, cross-sectional curves obtained from the three different sides of the indentation edges need to be measured (the right graphs in the Fig. 4). These curves confirm both that the pile-ups are not symmetrical around the indentation edges and that the height and width of the pile-ups differ from each other at the three different sides of the indentations. Table 2 gives the detailed maximum height of the pile-up ($h_{pile\text{-}up}$) along the directions of 1-3 (clearly seen in the right graph of Fig. 4d) in these four materials. There exists a tendency that the $h_{pile\text{-}up}$ would reach the maximum values as the grain size increases from 30 nm to 300 nm, and then decreases in the CG Cu. Besides that, there is another interesting result that the area of the pile-up around the indenters increases continuously as the grain size increasing.

Preprints (www.preprints.org) | NOT PEER-REVIEWED | Posted: 3 October 2017 doi:10.20944/preprints201710.0019.v1

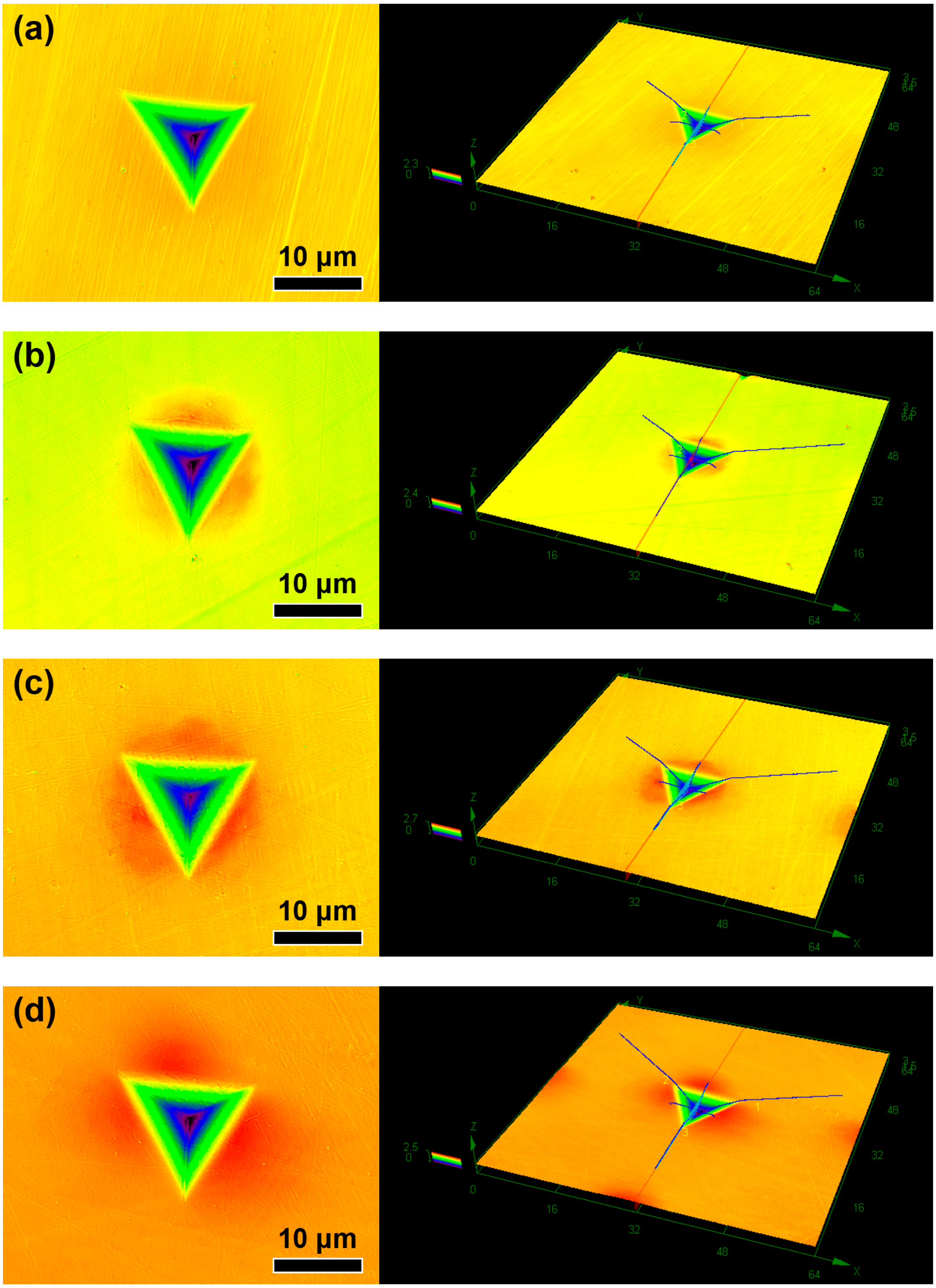

Fig.4 LCM images of 30 nm Cu (a), 150 nm Cu (b), 300 nm Cu (c) and CG Cu (d) obtained at strain rate of 0.04/s to the indentation depth of 2000 nm. The right is the corresponding three-dimensional graphs that can be used to measure the detailed height of the pile-up along the cross-section.

Table 2 $h_{pile\text{-}up}$ of NC/UFG/CG Cu at three directions.

Materials	$h_{pile\text{-}up}$ in the Direction 1	$h_{pile\text{-}up}$ in the Direction 2	$h_{pile\text{-}up}$ in the Direction 3

Preprints (www.preprints.org) | NOT PEER-REVIEWED | Posted: 3 October 2017 doi:10.20944/preprints201710.0019.v1

30 nm Cu	0.115 nm	0.099 nm	0.073 nm
150 nm Cu	0.228 nm	0.337 nm	0.292 nm
300 nm Cu	0.396 nm	0.386 nm	0.231 nm
CG Cu	0.244 nm	0.302 nm	0.227 nm

4. Discussion

Oliver-Pharr method is based on the pure elastic contact developed by Sneddon [17], and thus the tip calibration of the projected contact area at maximum load always considers sink-in effect occurring around the residual indenter, as shown in the Fig. 5. Finite Element Modeling (FEM) results have pointed out that [18], when the h_f/h_{max} is smaller than 0.7, or the materials have moderate work hardening, the Oliver-Pharr analysis procedure would provide a reasonable results of the measured *E* and *H*. When the h_f/h_{max} is larger than 0.7, and/or in the materials without obvious work harden, larger amount of the pile-up would directly induce an underestimation of the contact area, which further produces correspondingly large errors in the measurement (overestimation) of the *E* and *H*, especially at smaller indentation depth. Therefore, accurately determining the contact area from the *P-h* curves plays an important role in the measuring the mechanical properties of materials on a local small volume.

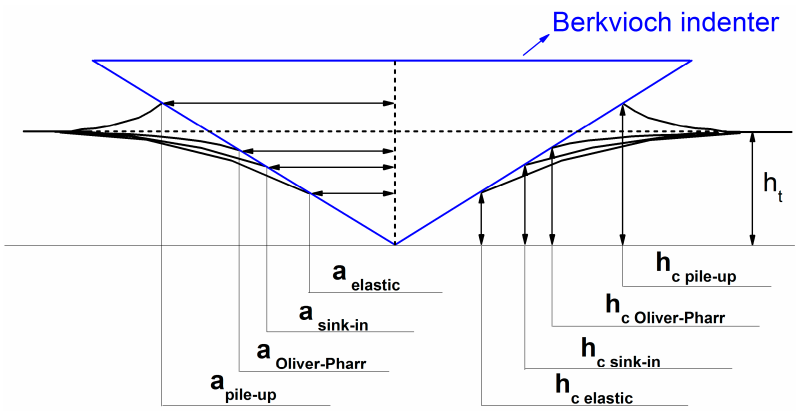

Fig. 5 Basic representation of pile up and sink in phenomena, a and h_c are the corresponding residual radius and contact depth.

The pile-up evolution during the indentation is closely related with the relative amounts of elastic and plastic deformation as characterized by the ratio of the elastic modulus to yield stress, i.e., E/σ_y. As $E/\sigma_y = 0$, the contact is strictly elastic and dominated by sink-in in the way prescribed by Hertzian contact mechanics. As $E/\sigma_y = \infty$, the indentation process follows the rigid-plastic deformation and extensive pile-up would occur around the residual impression [7]. Our previous reports have already studied systematically the tensile properties of the NC/UFG Cu with different grain sizes [14, 16, 19], and the corresponding values of E/σ_y in these four materials are 175 (30 nm Cu), 264 (150 nm Cu), 386 (300 nm Cu), 1930 (CG Cu). As expected, elastic behavior is larger for the NC Cu because of smaller h_f/h_{max} value, but there is little recovery for materials with larger grain size due to the fact that the sufficiently larger plasticity happens in these materials. Previous works are mostly focused on the new modified method to acquire more reliable measurement data in the nanoindentation. For example, direct measurement of the residual hardness impression could provide more accurate and believable contact area in evaluating the *E* and *H* [4, 6]. Very few studies concerns how the deformation mechanisms in the crystalline materials with different grain sizes influence the formation of the pile-up in the metal materials.

As the grain size further decreases below 100 nm, more GBs are involved in the indentation deformation and both dislocation activity and GB sliding can be activated in the strain rate range studied. In this case, large amount of slip planes are activated and dislocations emitted from GBs

 doi:10.20944/preprints201710.0019.v1

would propagate in the grain interior and be absorbed by the opposite GBs. This indicates that the highly mobile or unstable generated dislocations in the loading regime can only stay temporarily in grain interior, because GB serves as a sink for dislocation absorption, and the materials exhibit very limited strain hardening capability (as shown in Fig. 6a). Therefore, the effect of the pile-up induced by the strain hardening becomes invalid. Additionally, the changes of the grain shape can hardly happen in the plastic deformation of the NC metals under our experimental conditions. Our previous TEM observations of the NC Cu samples before and after deformation under compression testing have revealed, although the grain size have slightly difference under the assistance of GB activities and grains rotations [16], no obvious change of grain shape can be observed that could induce larger pile-up effect in the UFG metals.

As the grain size enters the ranges of 100~1500 nm, the dislocation density associated with grain boundaries becomes low, whereas the forest dislocation density in the grain interior is expected to become high. This deformation mechanism transition is consistent with the variation of m value versus grain size, which is in accordance with other experimental results of tensile, compression and nanoindentation testing [14, 16, 20-23]. Although a number of GB mechanisms such as GB sliding, GB rotation would participate in their plastic deformation, the transition between intragranular and intergranular deformation mechanism is not supposed to be abrupt. Dislocation activities such as the cross- and multiple-slips from the internal source can still be activated effectively in the large grain zones, and dislocations can be trapped inside the grains as a result of dislocation interactions between slip systems or with debris left by cross-slip. So some parts of the pile-up can formed in a way similar to that in the CG metals, where strain hardening induces the plastic deformation around the surface (see the below). Except that, larger grains under indenter would be stretched severely along the shear directions [24, 25] (as shown in Fig. 6b), which can also produce the highest $h_{pile\text{-}up}$ in the UFG Cu with grain size of 300 nm.

For the conventional CG metals, the plastic deformation mainly involves the dislocation multiplication from the intragranular Frank-Read sources, which could produce the dislocation cells/walls/networks structure in the grain interior. These formed microstructures as a strong pinning point to the dislocation-bowing segment would suppress dislocation cross slips, leading to strong strain hardening in the further plasticity. FEM results have revealed that due to the higher stress applied underneath the tip of the indenter, the shear strain or dislocation density generated at the deepest areas is much higher compared with other areas and materials around this region harden more severely [8]. The strain hardening generated by such dislocation activities is more effective in suppressing the strain localization. But for the regions approaching the surface, the dislocation slips in the other $<110>$ directions would become relatively easy that contributes to final the topography of the pile-up. Due to the relatively large strain hardening capability in the CG metals, larger regions around the surface would deform following the above mechanisms, producing larger areas of the pile-up (as shown in Fig. 6c).

 doi:10.20944/preprints201710.0019.v1

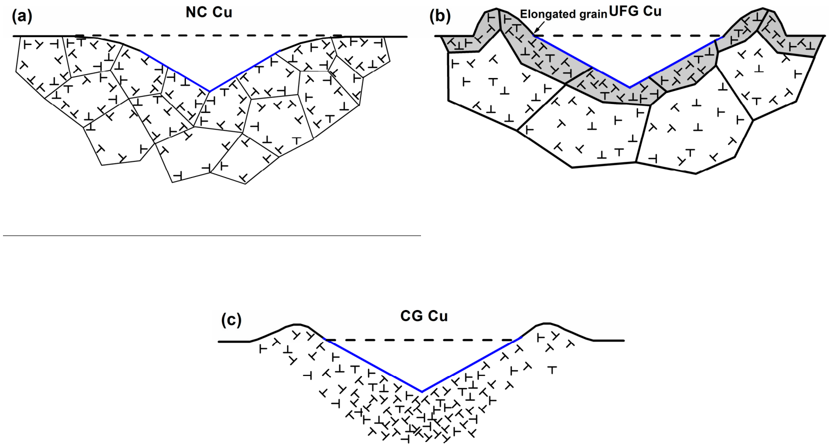

Fig. 6 Schematic illustrations of local GB structures and dislocation distribution in the NC (a), UFG (b) and CG (c) Cu underneath the indenters, where "T" represents dislocation.

5. Conclusion

Nanoindentation tests were carried out on crystalline Cu with different grain sizes ranging from 30 nm to 300 nm and CG Cu, and the residual indenter morphologies of these four materials have been systematically studied. It can be observed the height of the pile-up reaches the maximum values as the grain size increases from 30 nm to 300 nm, and then decreases in the CG Cu. Besides that, there is another interesting result that the area of the pile-up around the indenters increases continuously as the grain size increasing. Our analysis have demonstrated that dislocation activity and GB activities in the NC metals, some cross- and multiple-slips dislocation insides the larger grain in the UFG Cu, and forest dislocations from the intragranular Frank-Read sources in the CG Cu are responsible for the distinct pile-up effect in these materials.

Acknowledgement: This work was supported by the National Natural Science Foundation of China (Grant Nos. 11672356 and 11727803, 51371089) and Innovation team in key areas of Shaanxi Province (2016KCT-30).

Author Contributions: Jiangjiang Hu conducted the experiments and wrote the paper. Yusheng Zhang supervised the revised the whole work. Weiming Sun processed the data. Taihua Zhang conceived the work and also revised the paper.

Conflicts of Interest: The authors declare no conflict of interest.

References

1. Oliver, W.C., Pharra, G.M. Measurement of hardness and elastic modulus by instrumented indentation: Advances in understanding and refinements to methodology. *J. Mater. Res. 2004, 19, 3.*
2. McElhaney, K.W., Vlassak, J.J., Nix, W.D. Determination of indenter tip geometry and indentation contact area for depth-sensing indentation experiments. *J. Mater. Res. 1998, 13, 1300.*
3. Gale, J.D., Achuthan, A. The effect of work-hardening and pile-up on nanoindentation measurements. *J. Mater. Sci. 2014, 49, 5066-5075.*
4. Beegan, D., Chowdhury, S., Laugier, M.T. A nanoindentation study of copper films on oxidised silicon substrates. *Surf. Coat. Tech. 2003, 176, 124-130.*
5. Rodríguez, J., Maneiro, M.A.G. A procedure to prevent pile up effects on the analysis of spherical indentation data in elastic–plastic materials. *Mech. Mater. 2007, 39, 987-997.*
6. Zhou, L., Yao, Y. Single crystal bulk material micro/nano indentation hardness testing by nanoindentation instrument and AFM. *Mat. Sci. Eng. A 2007, 460-461, 95-100.*

Preprints (www.preprints.org) | NOT PEER-REVIEWED | Posted: 3 October 2017 doi:10.20944/preprints201710.0019.v1

7. Taljat, B., Pharr, G.M. Development of pile-up during spherical indentation of elastic–plastic solids. *Int. J. Solids. Struct. 2004, 41, 3891-3904*.
8. Liu, Y., Varghese, S., Ma, J., Yoshino, M., Lu, H., Komanduri, R. Orientation effects in nanoindentation of single crystal copper. *Int. J. Plasticity 2008, 24, 1990-2015*.
9. Demiral, M., Roy, A., El Sayed, T., Silberschmidt, V.V. Influence of strain gradients on lattice rotation in nano-indentation experiments: A numerical study. *Mat. Sci. Eng. A 2014, 608, 73-81*.
10. Sánchez-Martín, R., Pérez-Prado, M.T., Segurado, J., Molina-Aldareguia, J.M. Effect of indentation size on the nucleation and propagation of tensile twinning in pure magnesium. *Acta Mater. 2015, 93, 114-128*.
11. Renner, E., Gaillard, Y., Richard, F., Amiot, F., Delobelle, P. Sensitivity of the residual topography to single crystal plasticity parameters in Berkovich nanoindentation on FCC nickel. *Int. J. Plasticity 2016, 77, 118-140*.
12. Petryk, H., Stupkiewicz, S., Kucharski, S. On direct estimation of hardening exponent in crystal plasticity from the spherical indentation test. *Int. J. Solids. Struct. 2017, 112, 209-221*.
13. Chen, T., Tan, L., Lu, Z., Xu, H. The effect of grain orientation on nanoindentation behavior of model austenitic alloy Fe-20Cr-25Ni. *Acta Mater. 2017, 138, 83-91*.
14. Hu, J., Han, S., Sun, G., Sun, S., Jiang, Z., Wang, G., Lian, J. Effect of strain rate on tensile properties of electric brush-plated nanocrystalline copper. *Mat. Sci. Eng. A 2014, 618, 621-628*.
15. Hu, J., Sun, G., Zhang, X., Wang, G., Jiang, Z., Han, S., Zhang, J., Lian, J. Effects of loading strain rate and stacking fault energy on nanoindentation creep behaviors of nanocrystalline Cu, Ni-20 wt.%Fe and Ni. *J. Alloy. Compd. 2015, 647, 670-680*.
16. Hu, J., Zhang, J., Jiang, Z., Ding, X., Zhang, Y., Han, S., Sun, J., Lian, J. Plastic deformation behavior during unloading in compressive cyclic test of nanocrystalline copper. *Mat. Sci. Eng. A 2016, 651, 999-1009*.
17. Sneddon, I.N. The relation between load and penetration in the axisymmetric Boussinesq problem for a punch of arbitrary profile. *Int. J. Eng. Sci. 1965, 3, 47-57*.
18. Bolshakova, A., Pharr, G.M. Influences of pileup on the measurement of mechanical properties by load and depth sensing indentation techniques. *J. Mater. Res. 1998, 13, 4*.
19. Zhang, H., Jiang, Z., Lian, S., Jiang, Q. Strain rate dependence of tensile ductility in an electrodeposited Cu with ultrafine grain size. *Mat. Sci. Eng. A 2008, 479, 136-141*.
20. Li, H., Liang, Y., Zhao, L., Hu, J., Han, S., Lian, J. Mapping the strain-rate and grain-size dependence of deformation behaviors in nanocrystalline face-centered-cubic Ni and Ni-based alloys. *J. Alloy. Compd. 2017, 709, 566-574*.
21. Hu, J., Sun, W., Jiang, Z., Zhang, W., Lu, J., Huo, W., Zhang, Y., Zhang, P. Indentation size effect on hardness in the body-centered cubic coarse-grained and nanocrystalline tantalum. *Mat. Sci. Eng. A 2017, 686, 19-25*.
22. Hu, J., Zhang, W., Bi, G., Lu, J., Huo, W., Zhang, Y. Nanoindentation creep behavior of coarse-grained and ultrafine-grained pure magnesium and AZ31 alloy. *Mat. Sci. Eng. A 2017, 698, 348-355*.
23. Jiang, Z., Liu, X., Li, G., Jiang, Q., Lian, J. Strain rate sensitivity of a nanocrystalline Cu synthesized by electric brush plating. *Appl. Phys. Lett. 2006, 88, 143115*.
24. Wei, Q., Jia, D., Ramesh, K.T., Ma, E. Evolution and microstructure of shear bands in nanostructured Fe. *Appl. Phys. Lett. 2002, 81, 1240*.
25. Wei, Q., Kecskes, L., Jiao, T., Hartwig, K.T., Ramesh, K.T., Ma, E. Adiabatic shear banding in ultrafine-grained Fe processed by severe plastic deformation. *Acta Mater. 2004, 52, 1859-1869*.